

Ambipolar organic field-effect transistors based on a low band gap semiconductor with balanced hole and electron mobilities

Masayuki Chikamatsu,^{a)} Takefumi Mikami,^{b)} Jiro Chisaka, Yuji Yoshida, Reiko Azumi, and Kiyoshi Yase

Photonics Research Institute, National Institute of Advanced Industrial Science and Technology, Tsukuba Central 5, 1-1-1 Higashi, Tsukuba, Ibaraki 305-8565, Japan

Akihiro Shimizu, Takashi Kubo, Yasushi Morita, and Kazuhiro Nakasuji

Department of Chemistry, Graduate School of Science, Osaka University, 1-1 Machikaneyama, Toyonaka, Osaka 560-0043, Japan

(Received 24 May 2007; accepted 5 July 2007; published online 24 July 2007)

The authors have demonstrated the thin-film properties and the ambipolar transport of a delocalized singlet biradical hydrocarbon with two phenalenyl radical moieties (Ph₂-IDPL). The organic field-effect transistors (OFETs) based on Ph₂-IDPL exhibit ambipolar transport with balanced hole and electron mobilities in the order of 10⁻³ cm²/V s. The Ph₂-IDPL film is an organic semiconductor with a low band gap of 0.8 eV and has small injection barriers from gold electrodes to both the highest occupied molecular orbital and the lowest unoccupied molecular orbital. A complementary metal-oxide-semiconductor-like inverter using two identical Ph₂-IDPL based ambipolar OFETs shows a sharp inversion of the input voltage with high gain. © 2007 American Institute of Physics. [DOI: 10.1063/1.2766696]

Ambipolar carrier transporting materials have been attracting interest concerning not only fundamental science for organic semiconductor but also device application for light-emitting transistors¹ and complementary metal-oxide-semiconductor (CMOS)-like logic circuits.²⁻⁸ So far, ambipolar organic field-effect transistors (OFETs) have been realized by using blend^{2,3,9} or bilayer^{4,10-12} structure of two compounds (*p*-type and *n*-type materials), which transport holes in the highest occupied molecular orbital (HOMO) of a *p*-type material and electrons in the lowest unoccupied molecular orbital (LUMO) of a *n*-type material. Recently, ambipolar OFETs based on a single component semiconductor have been also reported.^{2,5-8,13-17} However, conventional organic semiconductors tend to exhibit ambipolar transport with unbalanced field-effect hole and electron mobilities: since band gaps of the semiconductors are relatively wide (~2 eV), large injection barrier between a metal electrode and either HOMO or LUMO level cannot be avoided. For realization of high-performance ambipolar OFETs with balanced hole and electron mobilities, it is necessary to develop low band gap semiconductors.^{2,8,15}

Kubo *et al.* reported synthesis, and crystal and electronic structures of a delocalized singlet biradical hydrocarbon [Ph₂-IDPL, see Fig. 1(a)],¹⁸ which was designed so as to possess a small HOMO-LUMO gap originating from phenalenyl radical electronic structure. The compound demonstrates a strong intermolecular interaction between two phenalenyl radical moieties and thus forms an electronic state of a molecular aggregate in the solid state, resulting in a low band gap semiconductor. From the result of the band-structure calculation, a single crystal of Ph₂-IDPL has an electronic structure with large bandwidths in both HOMO and LUMO (0.54 and 0.51 eV, respectively).¹⁸ Therefore,

Ph₂-IDPL would be expected to exhibit high-performance ambipolar transport with balanced hole and electron mobilities. Here, we report the thin-film properties and the ambipolar transport of Ph₂-IDPL. CMOS-like inverters based on ambipolar OFETs are also demonstrated.

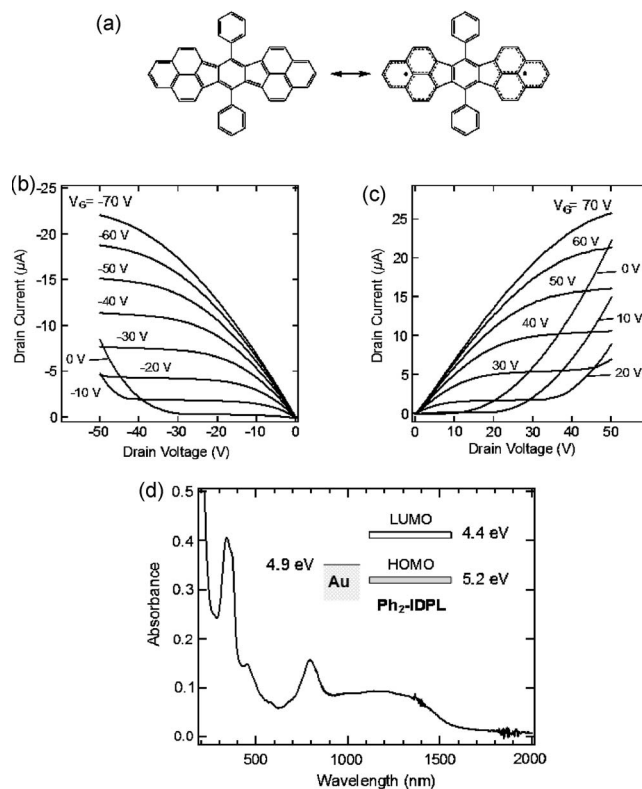


FIG. 1. (a) Resonance structures of Ph₂-IDPL. Output characteristics of the ambipolar OFET based on Ph₂-IDPL for (b) negative and (c) positive gate biases. (d) UV-visible-near IR spectrum of the Ph₂-IDPL film. The inset shows an energy band diagram of Ph₂-IDPL and Au. Ph₂-IDPL films were grown at a deposition rate of 0.2 Å/s and a substrate temperature of 25 °C.

^{a)}Electronic mail: m-chikamatsu@aist.go.jp

^{b)}Permanent address: Yamanashi Prefectural Industrial Technology Center, 2094 Ohtsu, Kofu, Yamanashi 400-0055, Japan.

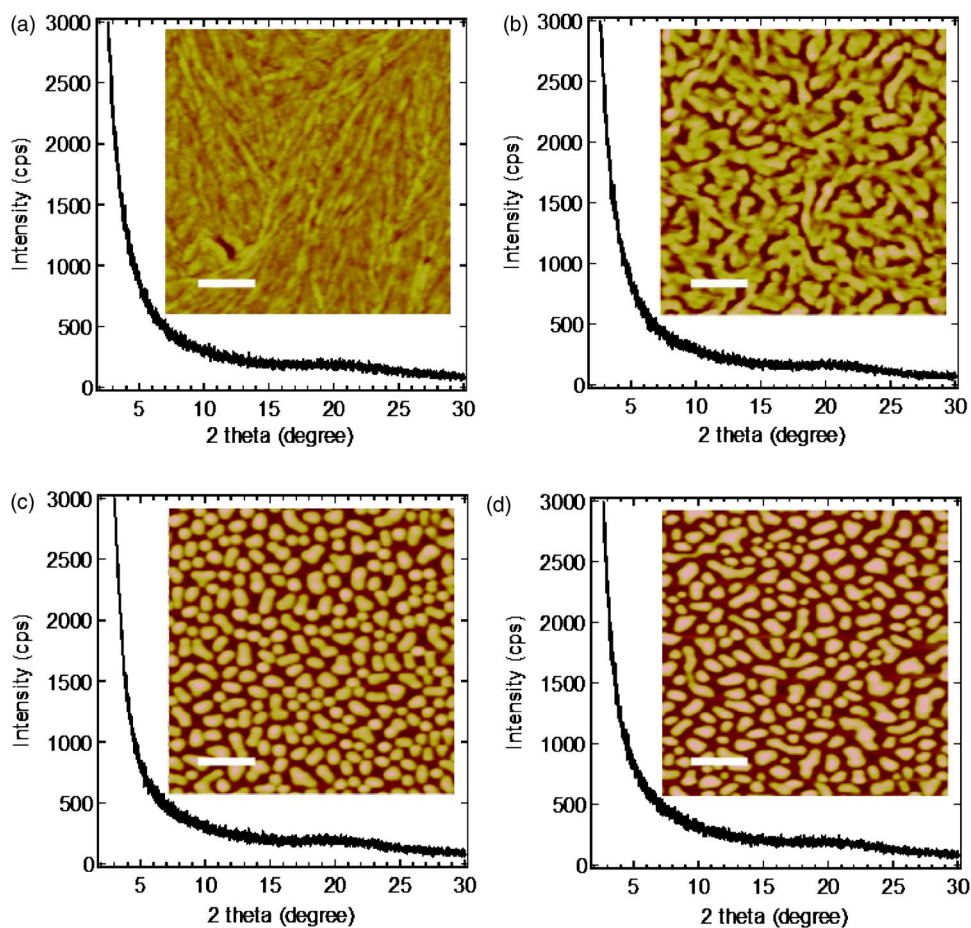


FIG. 2. (Color online) XRD patterns and AFM images (insets) of the Ph₂-IDPL films grown (a) at a deposition rate of 0.2 Å/s and T_{sub} of 25 °C, (b) at a deposition rate of 0.2 Å/s and T_{sub} of 60 °C, (c) at a deposition rate of 0.05 Å/s and T_{sub} of 60 °C, and (d) at a deposition rate of 0.09 Å/s and T_{sub} of 100 °C. The white scale bar in each AFM image corresponds to 1 μm .

The OFETs were constructed on a highly doped *n*-type silicon wafer covered with 300-nm-thick SiO₂ (a capacitance per unit area of 10 nF/cm²). The SiO₂ surface was treated with hexamethyldisilazane. Each film of Ph₂-IDPL was fabricated on the SiO₂ by vacuum evaporation under a pressure of 5×10^{-4} Pa. The thickness of each film is about 40 nm. Finally, gold source and drain electrodes were deposited on the films by using resistive heating evaporation source. A nickel thin plate, which was patterned with channel length (L) of 20 μm and channel width (W) of 5 mm, was used as a metal shadow mask. For the measurement of the OFET characteristics, Au wires were connected to the device electrodes using silver paste. The OFET characteristics were measured with Keithley 6430 and 2400 source measurement units in vacuum ($\sim 10^{-4}$ Pa). The field-effect mobility μ and the threshold voltage V_T were estimated from the square root of drain current-gate voltage ($I_D^{1/2}$ - V_G) plots, according to the standard equation in the saturation regime, $I_D = (W/2L) \mu C_i (V_G - V_T)^2$, where I_D is the drain current, W and L are the conduction channel width and length, respectively, C_i is the capacitance per unit area of the gate dielectric, and V_G is the gate voltage. X-ray diffraction (XRD) measurement of the films was carried out on a Rigaku Denki RU-300 using Cu $K\alpha$ radiation (40 kV, 200 mA) with a curved graphite monochromator. The diffractions were measured from 2° to 30° in the 2θ - θ scan mode with 0.01° step in 2θ and 0.6 s/step. An atomic force microscope (AFM) (Molecular Imaging Inc. MS300) operating in the contact mode was used to characterize the surface morphologies of the films.

Figures 1(b) and 1(c) show the *p*-channel and *n*-channel output characteristics of OFETs based on Ph₂-IDPL, respec-

tively. The Ph₂-IDPL film exhibits good ambipolar transport for both holes and electrons. The field-effect mobilities of hole (μ_h) and electron (μ_e) in saturation regime are calculated to be 2.6×10^{-3} and $3.2 \times 10^{-3} \text{cm}^2/\text{V s}$, respectively. The values of μ_h and μ_e are high compared with those of previously reported low band gap semiconductors (10^{-5} – $10^{-3} \text{cm}^2/\text{V s}$).^{2,8,15} It is also worth noting that the values of μ_h and μ_e are comparable with each other. The maximum on/off current ratios for both *p* and *n* channels reach 10^3 . After exposure to air, on current under *p*-channel operation was maintained, while on current under *n*-channel operation decreased by one order of magnitude compared with that in a vacuum.

Figure 1(d) shows an UV-visible-near IR absorption spectrum of the film. Sharp absorption peaks at 338 and 792 nm associated with intramolecular transition were observed. In addition, a broad peak around 1000–1500 nm associated with intermolecular transition was also observed. This can be explained by formation of the aggregate electronic state in the Ph₂-IDPL film. The band gap of Ph₂-IDPL was estimated to be 0.8 eV from the absorption onset. The energy band diagram of Ph₂-IDPL and gold is shown in Fig. 1(d) inset. The HOMO level of the Ph₂-IDPL aggregate was estimated to be 5.2 eV by photoelectron spectroscopy measurement (AC-2, Riken Keiki). The balanced hole and electron mobilities of the Ph₂-IDPL film seem to be due to the small injection barriers from the gold electrode (4.9 eV) (Ref. 19) to both HOMO and LUMO levels.

We investigated the film crystallinity and morphology of the film deposited at a substrate temperature (T_{sub}) of 25 °C by x-ray diffraction measurement and atomic force micro-

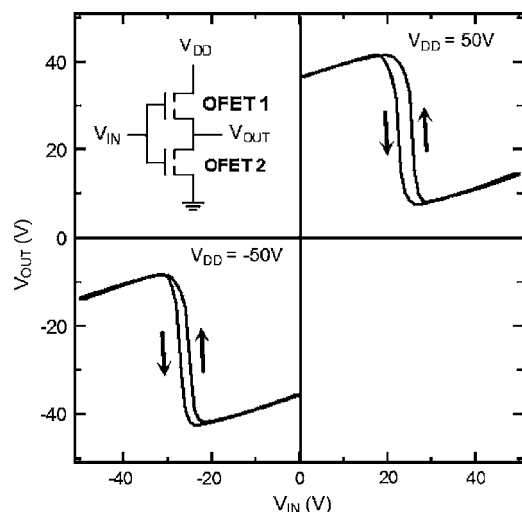


FIG. 3. Transfer characteristics of the CMOS-like inverter at supply voltages (V_{DD}) of +50 and -50 V. The inset shows the circuit configuration.

scope observation [Fig. 2(a)]. The results indicate that the film takes an amorphouslike structure without large crystalline domains. Therefore, we changed the deposition condition for optimizing the film structure. At T_{sub} of 60 °C, both hole and electron mobilities decrease by one order of magnitude ($\mu_h = 2.8 \times 10^{-4} \text{ cm}^2/\text{V s}$; $\mu_e = 3.0 \times 10^{-4} \text{ cm}^2/\text{V s}$) compared with those at $T_{sub} = 25$ °C. Moreover, as films are grown at a lower deposition rate (0.05–0.09 Å/s) and higher T_{sub} (60–100 °C), the OFETs demonstrate no active performance.

Thin-film growth of conventional π -conjugated oligomers tend to be improved as films are grown at a lower deposition rate and higher T_{sub} .^{20–22} In the case of Ph₂-IDPL, however, amorphous three-dimensional islands were grown at the condition of lower deposition rate and higher T_{sub} [Figs. 2(c) and 2(d)], resulting in no active performance of the OFETs based on Ph₂-IDPL. The results are due to strong intermolecular interaction of Ph₂-IDPL molecules compared with molecule-substrate interaction. The observed film morphology of Ph₂-IDPL is reminiscent of rubrene (C₄₂H₂₈) thin films.^{16,23} Rubrene also forms amorphous three-dimensional islands on a SiO₂ substrate, resulting in a low field-effect mobility ($\mu_h = \mu_e \approx 10^{-6} \text{ cm}^2/\text{V s}$) of the film,¹⁶ whereas single-crystal rubrene OFETs show a high hole mobility up to 20 cm²/V s.²⁴ Haemori *et al.* reported that rubrene thin-film growth is improved by surface modification of a substrate.²³ Therefore, further improvement of film crystallinity and mobility of Ph₂-IDPL can be expected by controlling molecule-substrate interaction. In addition, single-crystal Ph₂-IDPL is also expected to exhibit high hole and electron mobilities.

We have applied OFETs based on Ph₂-IDPL to a CMOS-like inverter, since the OFETs exhibit balanced ambipolar transport. Figure 3 shows transfer characteristics of the inverter, which was fabricated on a single substrate using two identical Ph₂-IDPL based ambipolar OFETs with a channel width of 5 mm and a length of 20 μm . Two ambipolar OFETs were connected to form an inverter with a common gate as the input voltage, V_{IN} (Fig. 3, inset). Sharp inversions of V_{IN} are observed with a high gain of 12 at half of the supplied voltage, V_{DD} (± 25 V). The symmetric inversions are

due to balanced hole and electron mobilities in the ambipolar OFETs. The inverter works in the first or the third quadrant: with the positive bias of V_{IN} and V_{DD} , OFET1 and OFET2 act as p - and n -type transistors, respectively, while OFET1 and OFET2 act as n - and p -type transistors under the negative bias condition of V_{IN} and V_{DD} . The behavior features ambipolar logic circuits.

In summary, we have demonstrated thin-film properties and ambipolar transport of Ph₂-IDPL. The OFETs based on Ph₂-IDPL exhibit good ambipolar transport with balanced hole and electron mobilities ($\mu_h = \mu_e \approx 3 \times 10^{-3} \text{ cm}^2/\text{V s}$). The Ph₂-IDPL film is an organic semiconductor with a low band gap of 0.8 eV and has small injection barriers from gold electrodes to both HOMO and LUMO. We found that Ph₂-IDPL is one of the promising organic semiconductors with high-performance ambipolar transport.

The authors thank S. Nagamatsu (Kyushu Institute of Technology) and A. Itakura for their assistance with the inverter measurement.

- ¹M. Muccini, *Nat. Mater.* **5**, 605 (2006).
- ²E. J. Meijer, D. M. de Leeuw, S. Setayesh, E. van Veenendaal, B.-H. Huisman, P. W. M. Blom, J. C. Hummelen, U. Scherf, and T. M. Klapwijk, *Nat. Mater.* **2**, 678 (2003).
- ³M. Shkunov, R. Simms, M. Heeney, S. Tierney, and I. McCulloch, *Adv. Mater. (Weinheim, Ger.)* **17**, 2608 (2005).
- ⁴H. Wang, J. Wang, X. Yan, J. Shi, H. Tian, Y. Geng, and D. Yan, *Appl. Phys. Lett.* **88**, 133508 (2006).
- ⁵T. D. Anthopoulos, D. M. de Leeuw, E. Cantatore, S. Setayesh, E. J. Meijer, C. Tanase, J. C. Hummelen, and P. W. M. Blom, *Appl. Phys. Lett.* **85**, 4205 (2004).
- ⁶T. D. Anthopoulos, D. M. de Leeuw, E. Cantatore, P. van't Hof, J. Alma, and J. C. Hummelen, *J. Appl. Phys.* **98**, 054503 (2005).
- ⁷Th. B. Singh, P. Senkarabacak, N. S. Sariciftci, A. Tanda, C. Lackner, R. Hagelauer, and G. Horowitz, *Appl. Phys. Lett.* **89**, 033512 (2006).
- ⁸T. D. Anthopoulos, S. Setayesh, E. Smits, M. Cölle, E. Cantatore, B. de Boer, P. W. M. Blom, and D. M. de Leeuw, *Adv. Mater. (Weinheim, Ger.)* **18**, 1900 (2006).
- ⁹K. Tada, H. Harada, and K. Yoshino, *Jpn. J. Appl. Phys., Part 2* **35**, L944 (1996).
- ¹⁰A. Dodabalapur, H. E. Katz, L. Torsi, and R. C. Haddon, *Science* **269**, 1560 (1995).
- ¹¹Y. Sakamoto, T. Suzuki, M. Kobayashi, Y. Gao, Y. Fukai, Y. Inoue, F. Sato, and S. Tokito, *J. Am. Chem. Soc.* **126**, 8138 (2004).
- ¹²E. Kuwahara, Y. Kubozono, T. Hosokawa, T. Nagano, K. Masunari, and A. Fujiwara, *Appl. Phys. Lett.* **85**, 4765 (2004).
- ¹³T. Yasuda, T. Goto, K. Fujita, and T. Tsutsui, *Appl. Phys. Lett.* **85**, 2098 (2004).
- ¹⁴Th. B. Singh, F. Meghdadi, S. Günes, N. Marjanovic, G. Horowitz, P. Lang, S. Bauer, and N. S. Sariciftci, *Adv. Mater. (Weinheim, Ger.)* **17**, 2315 (2005).
- ¹⁵T. Yasuda and T. Tsutsui, *Jpn. J. Appl. Phys., Part 2* **45**, L595 (2006).
- ¹⁶S. Seo, B.-N. Park, and P. G. Evans, *Appl. Phys. Lett.* **88**, 232114 (2006).
- ¹⁷T. Nishikawa, S. Kobayashi, T. Nakanowatari, T. Mitani, T. Shimoda, Y. Kubozono, G. Yamamoto, H. Ishii, M. Niwano, and Y. Iwasa, *J. Appl. Phys.* **97**, 104509 (2005).
- ¹⁸T. Kubo, A. Shimizu, M. Sakamoto, M. Uruichi, K. Yakushi, M. Nakano, D. Shiomi, K. Sato, T. Takui, Y. Morita, and K. Nakasuji, *Angew. Chem., Int. Ed.* **44**, 6564 (2005).
- ¹⁹B. de Boer, A. Hadipour, M. M. Mandoc, T. van Woudenberg, and P. W. M. Blom, *Adv. Mater. (Weinheim, Ger.)* **17**, 621 (2005).
- ²⁰M. Shtein, J. Mapel, J. B. Benziger, and S. R. Forrest, *Appl. Phys. Lett.* **81**, 268 (2002).
- ²¹G. Horowitz and M. E. Hajlaoui, *Synth. Met.* **122**, 185 (2001).
- ²²S. Nagamatsu, K. Kaneto, R. Azumi, M. Matsumoto, Y. Yoshida, and K. Yase, *J. Phys. Chem. B* **109**, 9374 (2005).
- ²³M. Haemori, J. Yamaguchi, S. Yaginuma, K. Itaka, and H. Koinuma, *Jpn. J. Appl. Phys., Part 1* **44**, 3740 (2005).
- ²⁴V. Podzorov, E. Menard, A. Borissov, V. Kiryukhin, J. A. Rogers, and M. E. Gurskens, *Phys. Rev. Lett.* **93**, 086602 (2004).